Supporting Information

Regulation of Photovoltaic Response in ZSO-based Multiferroic BFCO/BFCNT Heterojunction Photoelectrodes via Magnetization and Polarization

Kaixin Guo, [†] Rongfen Zhang,[†] Zhao Fu,[‡] Liangyu Zhang,[‡] Xu Wang,[†] and Chaoyong Deng[*,†]

†*Key laboratory of Electronic Composites of Guizhou Province, College of Big Data and Information Engineering, Guizhou University, Guiyang 550025, Guizhou, China;*

‡*Guizhou College of Electronic Science and Technology, Guiyang 561113, Guizhou, China*

* Author to whom correspondence should be addressed: cydeng@gzu.edu.cn.

Table of contents

1. Preparation and Characterization

Precursor Synthesis

Precursor of the electron transport layer (ZSO). The ZSO solution was prepared by adding 2 mmol of ethanolamine into a mixture of 2 mL 2-methoxyethanol, 1 mmol of $Zn(Ac)_2{\cdot}2H_2O$ and 0.5 mmol of $Sn(Ac)_4$. After stirring at 125°C for 1 h. The solution were then aged at room temperature for 48h to get the Zn_2SnO_4 precursor.

Precursor of the active layer. The BFCO solution (30 ml, 0.15 M) and BFCNT (50 ml, 0.03 M) were prepared by chelating the needed metallic nitrate with $C_5H_8O_2$ in a mixture of $C_2H_4O_2$ and appropriate $C_3H_8O_2$ at 50°C for 4 h. The solution were then aged at room temperature for 48h to get the corresponding precursors.

Device Fabrication.

The BFCO layers was first spin-coated onto the cleaned FTO at 3000 r.p.m. followed with an annealing at 500°C for 600s in air, repeated three times to get the required thickness, then the BFCNT lamina was deposited onto the BFCO in the same way, thus forming the tandem active layer. Next, the Zn_2SnO_4 layer was prepared by spin-coating the diluted Zn_2SnO_4 sol with ethanol (w:w = 1:5) about 30s at 3000 r.p.m. and annealing at 500°C for 600 s in air. In the end, the Pt electrodes were sputtered using a shadow mask.

Characterization

The phase structure information was determined by an X-ray diffractometer (XRD, SmartLab XG, Rigaku) with Cu Kα monochromatic radiation (λ = 1.54 18 Å) at a scanning speed of 2° min^{-1} in steps of 0.02°. The microstructure was obtained via a field emission scanning electron microscope (SEM, Regulus 8100, Hitachi). The Femi energies and valence band edges of the materials were determined by ultraviolet photoelectron spectroscopy (UPS, Escalab 250Xi, Thermo fisher). The optical measurements of the films were investigated by a UV spectrophotometer (U-4100, Hitachi) working in the ultraviolet-visible-near infrared (UV-Vis-NIR) range. The ferroelectricity and the corresponding ferromagnetism were analyzed by a multiferroic test system (Multiferroic 200V, Radiant Technologies) and a physical property measurement system (PPMS, DynaCool-9, Quantum Design™), respectively. The macroscopic magnetoelectric coupling was characterized in an open circuit condition in a self-assembly system. The Current-Voltage measurements were performed using a solar simulator (96000, Newpret-Stratfort 150W) with simulated AM 1.5 spectrum and power density of 100 $mW \cdot cm^{-2}$.

2. Phase Compositions and microtostructure

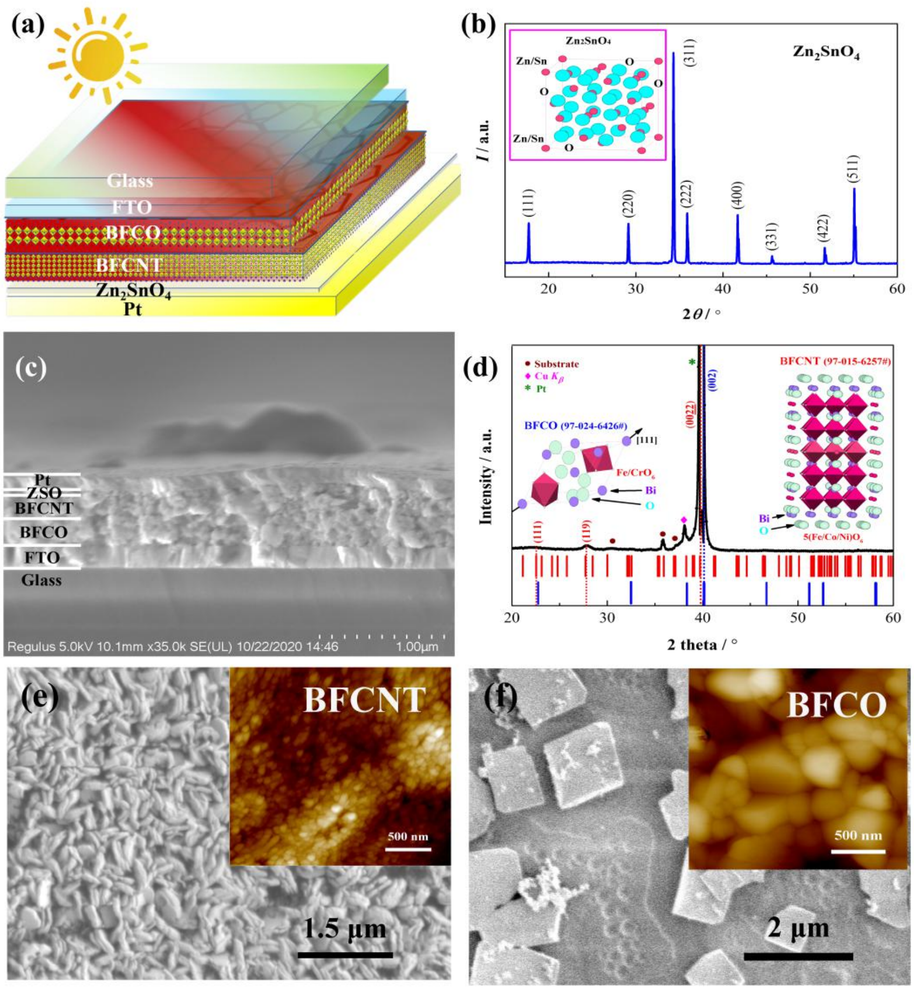

Figure S1. Microstructure, crystal texture and XRD pattern. (a) Schematic of the multiferroic solar cell, (b) XRD pattern and the unit cell structure of ZSO, (c) SEM images of both the full device stack, (d) XRD pattern and the unit cell structures of BFCO/BFCNT heterojunction, (e) and (f) Microstructures of BFCNT and BFCO layers.

3. Multiferroic properties

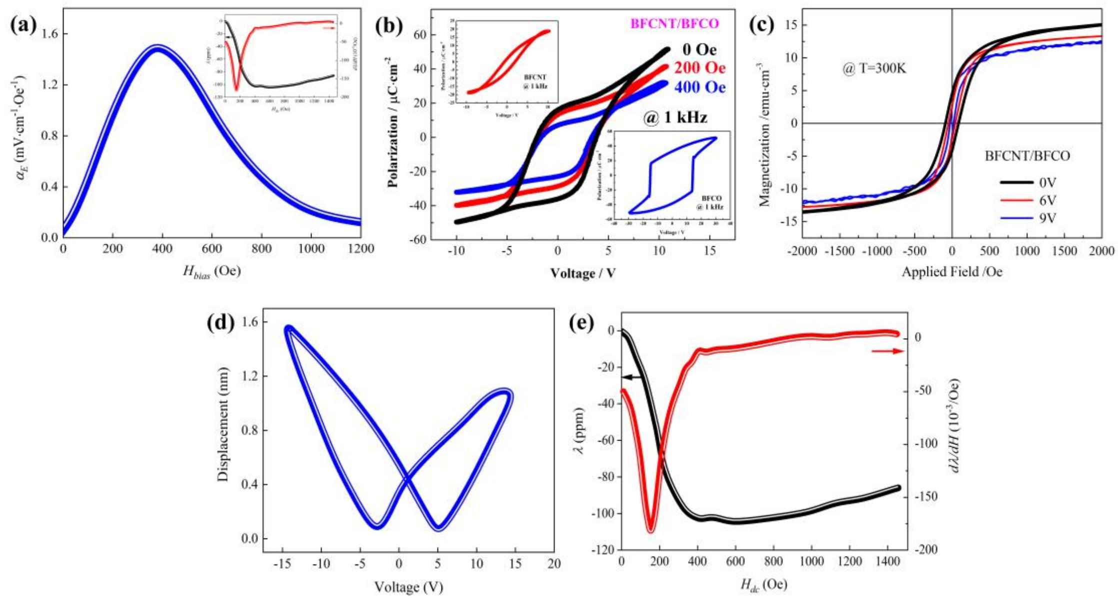

Fig. S2. **Magnetoelectric coupling of multiferroic BFCO/BFCNT heterojunction.**

(a) Magnetoelectric coupling effect, (b) Magnetic field regulated polarization reversal, (c) Voltage regulated magnetization reversal, (d) and (e) Piezoelectric and magnetostriction effect.

Materials that have combined different performances of ferroic orders such as (anti-)ferromagnetism, (anti-)ferroelectricity and (anti-)ferroelasticity simultaneously are known as multiferroics. These multiferroics show opportunities for promising applications in information storage, sensors, spintronic and actuator devices [1-4]. The magnetoelectric coupling effect (α) is essentially the stress induced by a magnetostriction resulted from the magnetic field is transmitted to the piezoelectric phase by means of the piezoelectric effect, resulting in an induced electric field. It is virtually a product of composite materials, *i.e.* $\alpha = \frac{H}{S} \times \frac{S}{E}$ [5], where S refers to the strain, H and E are magnetic and electric field, respectively.

Once a constant magnetic field is applied to multiferroic materials, the materials will stretch along the magnetic field direction due to the magnetostrictive effect, causing a shrinkage to some extent in the other two directions. This stress will be transferred to the piezoelectric phase mainly through the interface due to the magnetoelectric coupling effect, resulting in a corresponding longitudinal deformation, *i.e*. the regulation of magnetic field on electrical properties, which is just the positive magnetoelectric effect. On the contrary, the tuning of magnetism by an applied electric field is the inverse magnetoelectric effect.

Reference:

[1] Eerenstein, W.; Mathur, N. D.; Scott, J. F. Multiferroic and magnetoelectric materials. *Nature*, **2006**, *442*, 759-765.

[2] Cheong, S. W.; Mostovoy, M. Multiferroics: a magnetic twist for ferroelectricity. *Nat. Mater*. **2007**, *6*, 13-20.

[3] Liu, Y. Y.; Li, J. Y. Multiferroics: Looking back and going forward. *Sci. China Technol. Sc*. **2020**, *63*, 1-2.

[4] Scott, J. F.; Evans, D. M.; Gregg, J. M.; Gruverman, A. Hydrodynamics of domain walls in ferroelectrics and multiferroics: impact on memory devices. *Appl. Phys. Lett*. **2016**, *109*, 042901.

[5] Nan, C. W.; Bichurin, M. I.; Dong, S.; Viehland, D.; Srinivasan, G. J. Multiferroic magnetoelectric composites: historical perspective, status, and future directions. *J. Appl. Phys*. **2008**, *103*, 031101.

4. The optical properties

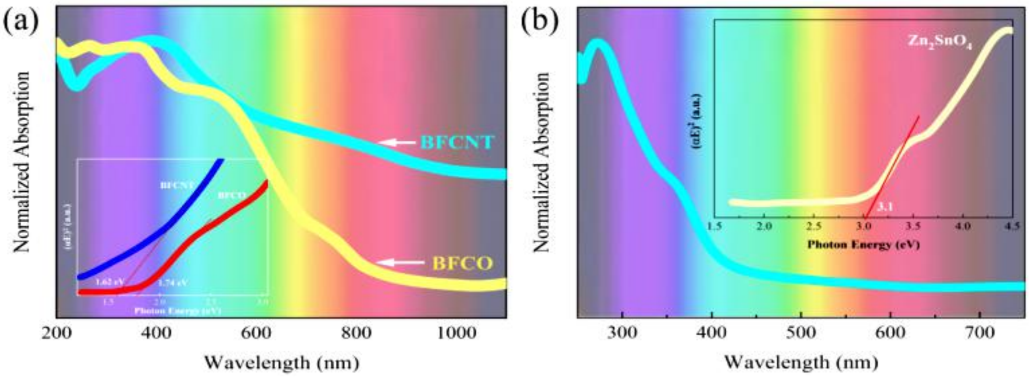

Figure S3. UV-Vis-NIR spectra of BFCO, BFCNT and ZSO. The *insets* are the corresponding $(\alpha E)^2$ versus energy plots.

Table S1. UPS results of each layer of the device.

No.	Materials	CBM (eV)	VBM (eV)
1	BFCO	-3.6	-5.3
2	BFCNT	-3.8	-5.4
3	ZSO	-4.2	-7.3

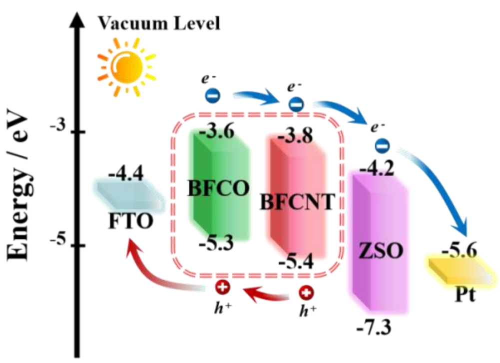

Fig. S4. **Energy-level diagram based on UPS results.**

5. Photovoltaic properties

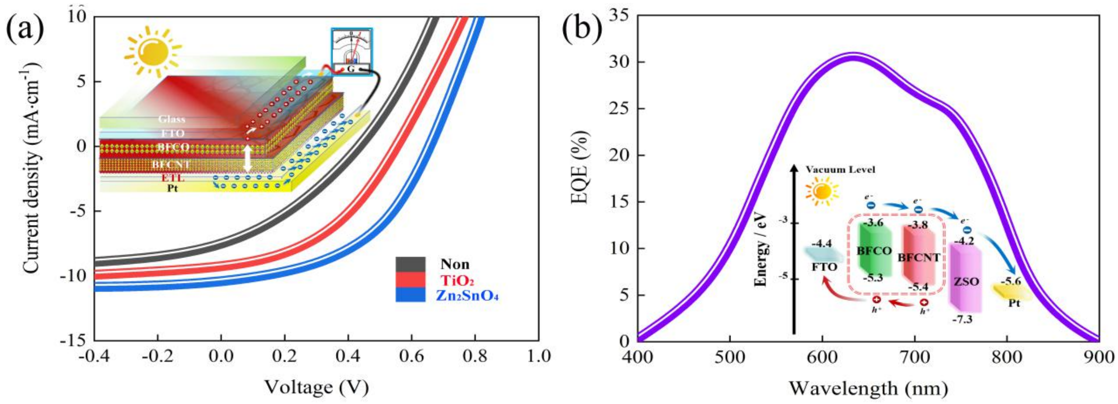

Figure S5. The optical and photovoltaic properties. (a) *J-V* characteristic under AM 1.5G illumination of the solar cell, (b) External quantum eficiency of the photovoltaic device.